Materials Science & Engineering A 691 (2017) 150–154

Contents lists available at ScienceDirect

Materials Science & Engineering A

journal homepage: www.elsevier.com/locate/msea

Effect of sample orientation and initial microstructures on the dynamic recrystallization of a Magnesium alloy

P. Gao[a], S.Q. Zhu[a], X.H. An[a], S.Q. Xu[b], D. Ruan[c], C. Chen[d], H.G. Yan[d], S.P. Ringer[a,e], X.Z. Liao[a,*]

[a] School of Aerospace, Mechanical & Mechatronic Engineering, The University of Sydney, Sydney, NSW 2006, Australia
[b] Centre for Innovative Structures and Materials, School of Engineering, RMIT University, Melbourne, VIC 3000, Australia
[c] Faculty of Science, Engineering and Technology, Swinburne University of Technology, Hawthorn, VIC 3122, Australia
[d] College of Materials Science and Engineering, Hunan University, Changsha 410082, China
[e] Australian Institute for Nanoscale Science and Technology, The University of Sydney, NSW 2006, Australia

ARTICLE INFO

Keywords:
Magnesium alloys
Grain orientation
Dynamic recrystallization
Twinning
Dislocation

ABSTRACT

Strongly textured Mg–3Al–1Zn (wt%) alloy samples with a high density of twins cut from three directions were used to investigate the effect of crystallographic orientation on dynamic recrystallization (DRX). The samples were deformed under a high strain rate at 300 °C. The high strain rate allows rapid dislocation accumulation, making DRX possible at relatively low strain values. We demonstrate that crystallographic orientation and the initial twins have significant effects on DRX because of the different activities of dislocations and their interactions with twin boundaries. This research provides a potential pathway for improving the formability of Mg alloys.

1. Introduction

Due to their lightweight and high specific strength, Mg alloys have been extensively investigated as promising structural materials [1–4]. However, poor formability at low temperatures has been a major obstacle limiting their widespread applications [5–7]. Recent investigations indicated that plastic deformation of Mg alloys at relatively high strain rates (~50 s^{-1}) at temperatures of > 250 °C promotes dynamic recrystallization (DRX) and this substantially improves both the formability and mechanical properties [8]. Increasing the strain rate of deformation promotes deformation twinning and the accumulation of dislocations in areas near twin boundaries (TBs). The high densities of accumulated dislocations lead to very high stored energies, triggering DRX. This reduces the local stored energy and facilitates further deformation [8]. It is interesting to note that the DRX process did not occur uniformly throughout the microstructures [8,9] and this was thought to be related to the orientation dependence that affected the deformation behaviour. This work explores that dependence.

Grain orientation determines the Schmid factors of slip systems. This affects the deformation mechanisms [10,11] and consequently dislocation densities and dislocation-TB interactions that have a significant effect on the potential for DRX in Mg alloys [12–14]. Just how grain orientation can affect DRX remains unclear, however. The effect of initial twins on DRX under various orientations is also largely unknown. This study aimed to use a strongly textured Mg alloy with a high density of twins to explore how grain orientation and initial twins affect DRX behaviour at elevated temperature. High strain-rate deformation was used in the study because this allows rapid dislocation accumulation [15–17] and makes deformation twinning easy [18,19], which enables DRX at relatively low strain values.

2. Materials and experimental procedures

An as-cast AZ31 (Mg–3Al–1Zn, in wt%) Mg alloy was used in this study. The Mg alloy ingot with an initial thickness of 25 mm was hot pressed by 5 passes at 250 °C. With a thickness reduction of 1 mm per pass, the final thickness was reduced to 20 mm. The as-pressed plate was then annealed at 150 °C for 30 min to relieve the internal stress. Cylindrical samples with a diameter of 11.6 mm and a height of also 11.6 mm were cut in three ways as demonstrated in Fig. 1 so that the axial direction of the samples was parallel to (i) the normal direction, (ii) 45° away from the normal direction, and (iii) perpendicular to the normal direction of the plate. These samples are hereafter referred to as ND, 45ND and 90ND samples, respectively.

X-ray diffraction (XRD) for macroscopic texture analysis was carried out using a Shimadzu S6000 X-ray diffractometer. High strain-rate compression was performed along the cylindrical axial direction at 300 °C using a maraging steel Split Hopkinson Pressure

* Corresponding author.
E-mail address: xiaozhou.liao@sydney.edu.au (X.Z. Liao).

http://dx.doi.org/10.1016/j.msea.2017.03.047
Received 6 January 2017; Accepted 10 March 2017
Available online 12 March 2017
0921-5093/

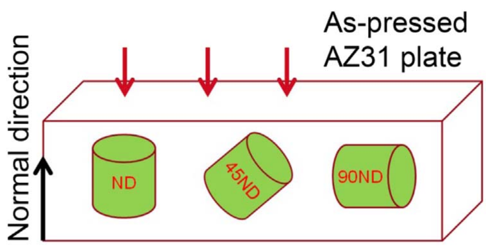

Fig. 1. Sampling methods from the as-pressed AZ31 plate.

Bar (SHPB) apparatus at a strain rate of ~1000 s^{-1}. The heating process before SHPB took ~5–10 min, which brought no noticeable variation in the microstructure (see the Supplementary Material Fig. S1). At least four tests were conducted for each type of samples to ensure reproducibility of the stress–strain curve. Plan-view and cross-sectional microstructural characterisation was conducted before and after deformation using the electron backscatter diffraction (EBSD) technique in a Zeiss Ultra field emission scanning electron microscope working at 20 kV. The scanning step size was 1 μm and 0.7 μm for samples before and after deformation, respectively. The microstructural data were recorded by Aztec and analysed using Channel 5 software (*HKL* Technology) to acquire detailed information on grain orientation, boundary characteristics and to identify grains with internal misorientation smaller than 1°. It has been well accepted that grains with low internal misorientation are regarded as recrystallized grains [20–24].

3. Results and discussion

Fig. 2 shows typical high strain-rate compression true stress–strain curves of the three types of samples. The ND curve illustrates a concave down shape, which has been explained to be caused by dislocation slip [20]. The 45ND curve exhibits a low yield stress and a concave up shape immediately after yielding. However, the 45ND curve at later deformation stages resembles the ND curve. The first half of the 90ND strain–stress curve presents a concave up shape, which is indicative of the operation of tension twinning [20,25,26]. The yield stress of the ND, 45ND and 90ND samples presented in the figure was 146 MPa, 131 MPa and 130 MPa, respectively. The highest stress for ND, 45ND and 90ND samples was 213 MPa, 217 MPa and 286 MPa, respectively. The deformation strain for all samples was ~0.14. None of the samples was compressed to fracture.

Fig. 3 illustrates the microstructure, texture and grain boundary misorientations of the material before high strain-rate deformation. Combined optical (not shown here) and electron microscopy observations revealed that the grain sizes covered a large range from tens of microns to ~300 μm. This research focuses on the collective effect of the overall microstructure that includes both fine and coarse grains.

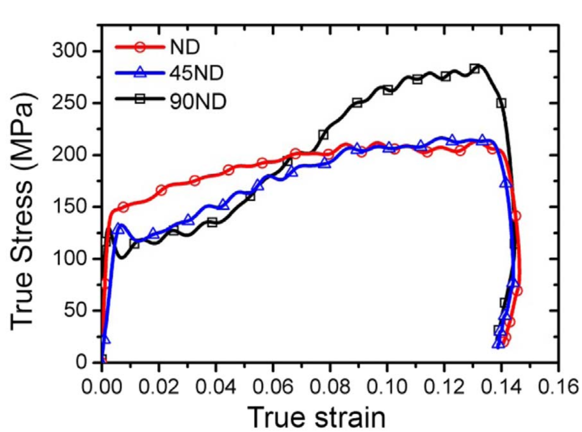

Fig. 2. True stress–strain curves from SHPB testing.

Fig. 3a presents an EBSD inverse pole figure (IPF) map observed from the Normal direction. A large statistics area was examined, which presented the typical structure of the sample. Strong [0001] basal texture with most c-axes appropriately parallel to the Normal direction was evident. Because of their sampling methods, grains in the ND, 45ND and 90ND samples had most of their c-axes oriented approximately 0°, 45° and 90° away from the sample axial direction, respectively. These were consistent with the XRD results in Fig. 3b that show the strongest peak in (0002) diffraction for ND, $(10\bar{1}1)$ for 45ND, and $(10\bar{1}0)$ and $(10\bar{1}1)$ for 90ND. Fig. 3c displays the distribution of grain boundary misorientations. Low-angle grain boundaries with misorientation angles ~2–10° took up about 28% of the total grain boundaries. Two peaks presented at 38° and 86° are from $\{10\bar{1}1\}-\{10\bar{1}2\}$ double twins (with a misorientation of 38° at TBs around a $<1\bar{2}10>$ axis) and $\{10\bar{1}2\}$ tension twins (with a misorientation of 86° at TBs around a $<1\bar{2}10>$ axis) [25,27], respectively.

Fig. 4 shows the microstructures of the three types of samples after high strain-rate deformation. The high strain-rate deformation led to grain reorientation in such a way that the [0001] of most grains was approximately parallel to the surface normal of the deformed samples (or the loading direction of the deformation), as demonstrated by the EBSD pole figures inset in Fig. 4a–c. This implies that the c-axis of grains in 45ND and 90ND was generally tilted ~45° and ~90° towards the loading direction, respectively, while the c-axis of most grains in ND samples remained parallel to the loading direction throughout the deformation process. The distribution of DRX grains is presented in Fig. 4d–f. Image analysis of large areas revealed that the volume fraction of DRX in the ND, 45ND and 90ND samples was 63%, 51% and 3.7%, respectively. Careful examination of areas with low degrees of DRX in ND and 45ND samples indicated that the DRX occurred preferentially in the twinned areas. The arrows in Fig. 4d and e, reveal parallel DRX striped regions. The striped areas were twinned regions prior to DRX. This observation is consistent with the previous reports that twins are preferred DRX sites [8] because they serve as effective obstacles for dislocation motion, leading to significant dislocation accumulation around the TBs [8,28]. Indeed, numerous small-angle grain boundaries, which is indicative of a high density of dislocations [8], were observed in twinned areas where DRX had not occurred. An example is highlighted with a black rectangle in Fig. 4d and its magnified image is inset at the lower left corner of the figure. These experimental observations suggest that extensive dislocation activities and local dislocation accumulation at TBs are critical to enable DRX.

Quantitative results of the volume fractions of DRX regions, relative frequencies of grain boundary misorientations, and average grain sizes before and after SHPB testing for all three sample orientations are listed in Table 1. The much larger degrees of DRX in ND and 45ND than in 90ND coincide with the fact that the ND and 45 ND samples had much smaller relative frequencies for low-angle grain boundaries and much smaller average grain sizes than 90 ND. Note that in addition to DRX, combined significant dislocation activities and deformation twinning also leads to remarkable grain refinement [29–31]. Because of the relatively high dislocation densities, the grain refinement in 90ND was mainly introduced by plastic deformation. Twin densities, which can be reflected by the relative frequencies of 38°, 56° and 86° grain boundaries, in ND and 45ND were lower than those in 90ND. One reason is that DRX effectively eliminated TBs.

DRX in Mg alloys is promoted by high densities of dislocations [32–34]. Deformation modes, including slip and twinning, play a crucial role in the subsequent DRX during high temperature deformation [9]. Critical resolved shear stress (CRSS) and Schmid factor are very important in determining the deformation mechanisms. Because of the strong texture of the material, the plane normal of most basal planes of the grains in the ND, 45ND and 90ND samples before high SHPB testing was close to 0°, 45° and 90° away from the loading direction. Admittedly, there were basal plane poles titled in the material before processing. Because the material was polycrystalline